CATALOGUE CORRELATION OF SPACE DEBRIS OBJECTS

Carolin Früh[1], Thomas Schildknecht[2], Reto Musci[3], Martin Ploner[4]

Astronomical Institute, University of Bern, Sidlerstrasse 5, 3012 Bern, Switzerland,
[1]frueh@aiub.unibe.ch, [2]schildknecht@aiub.unibe.ch, [3]musci@aiub.unibe.ch, [4]ploner@aiub.unibe.ch

ABSTRACT

One important step when performing surveys of space debris objects is to correlate each actual detection of an object with one or several catalogues of known objects. Usually the output of optical surveys is a short series of astrometric positions for each detection, also called a tracklet, spanning an interval of a few minutes. Single tracklets do not allow to determine a six parameter orbit.

This paper describes a new method to correlate observed space debris objects with internal and external catalogues by comparing the observed and the computed topocentric positions and velocities. Since official catalogues like DISCOS do not provide covariance information, the catalogue errors have been assessed by comparing observed and the computed positions and velocities of a set of known objects.

The new correlation method is applied to typical GEO and GTO survey observations from the ESA Space Debris Telescope (ESASDT) on Tenerife. In addition first results of the application of the method to the surveys of the ZimSMART wide field telescope in Zimmerwald, Switzerland, are presented.

1 INTRODUCTION

For several years now the Astronomical Institute of the University of Bern (AIUB) has been performing observations using the 1 m ESA Space Debris Telescope (ESASDT) on Tenerife, Canary Islands, and follow-up observations with the 1 m telescope ZIMLAT, located close to Bern, Switzerland, with the aim to gain statistical information of the space debris population in the geostationary ring (GEO) and in geostationary transfer orbits (GTO).

One important step in the automatic processing of the data of the ESASDT is to correlate the observed short series of two to eleven astrometric positions, also called tracklets with a catalogue. This task is especially demanding, since the tracklets span only intervals of a few minutes, which does not allow to determine a full six parameter orbit, as explained in detail in [1]. A circular orbit is determined instead. The old algorithm, which has been used previously in the automatic processing, performs the catalogue correlation by comparing orbital elements. A circular orbit is a good approximation for GEO objects, whose orbits have very small eccentricities. But it is a bad approximation for GTO orbits. Details how tracklets of object in orbits with non-vanishing eccentricity are represented in a circular first orbit determination can be found in [2]. This makes it impossible to correlate with the old algorithm others than tracklets of objects on orbits with vanishing eccentricity.

A new algorithm has been developed, which compares the observed apparent topocentric positions and apparent velocities with computed positions and velocities from internal catalogues and the DISCOS catalogue. Since no covariance information is given in DISCOS, catalogue errors are assessed by comparing computed ephemerides with tracklets of known objects. These tracklets stem from follow-up observations of GEO and GTO objects, observed with the ZIMLAT, or from GEO objects, observed in surveys with the ESASDT. The results of the new algorithm are validated in the first case by orbit determination and in the latter by comparing with the results of the old algorithm.

The performance of the new algorithm was tested by reprocessing the ESASDT campaigns of January to March 2008 and by processing of satellite cluster observations observed with the 18 cm wide field telescope ZimSMART, located next to the ZIMLAT.

2 ASSESSMENT OF CATALOGUE ERRORS

2.1 Methods of error assessment

To assess the errors of catalogues, which do not provide covariance information, the ephemeris of catalogue objects are compared to the apparent positions and velocities of observed objects. The position error, called arc length error in this paper, is computed as

Proc. '5th European Conference on Space Debris', Darmstadt, Germany
30 March – 2 April 2009, (ESA SP-672, July 2009)

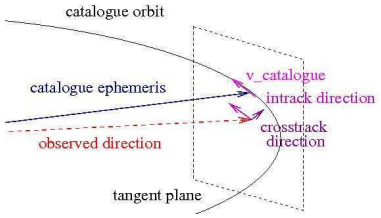

Figure 1: Catalogue and observed position under the assumption of common radial distance with intrack and crosstrack direction in tangent plane.

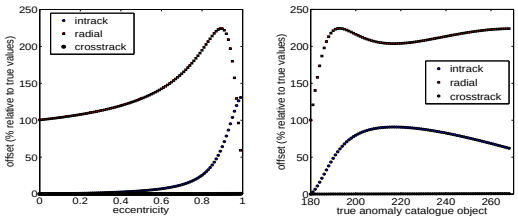

(a) *(b)*

Figure 2: Systematic offsets in percent relative to the "true" errors intrack, crosstrack and radial (NTW system) as a function of eccentricity (a) and true anomaly (b) assuming a common radial distance.

the angular distance between the observed position and the ephemeris. The intrack error is determined as the total offset between the observed and calculated position in direction of the velocity of the catalogue object projected in the tangent plane with origin in the observed object's position. The error orthogonal to the intrack direction in the tangent plane is called crosstrack error in this paper; it is the sum of the crosstrack error and the radial error in a NTW system (see [3] for details) projected in the tangent plane.

But these can only be expressed in angular distances, since optical observations provide only information about the direction of the observed object, not about the radial distance. The latter can only be gained by orbit determination from which the new algorithm should be independent of for reasons mentioned above. To obtain absolute values the radial distance of the observed object has to be approximated.

One method to approximate the radial distance is to assume that the radial distance of the observed object is the same as the one calculated for the catalogue object at the observation epoch. This setup is illustrated in Fig.1.

To assess the systematic offsets introduced by this assumption the following simulation setup is made: An artificial object on an orbit with a semi major axis of 24 000 km and inclination zero is observed from the geocenter. The geocenter is chosen to eliminate parallax effects. The position of the simulated observed object is shifted relative to the simulated catalogue position 60 kilometer in intrack direction, 20 kilometer in crosstrack direction and 20 kilometer in radial direction in a NTW system. In Fig.2a the offsets introduced by the assumption that the simulated observed object has the same radial distance than the simulated catalogue object in intrack, crosstrack and radial direction as a function of the eccentricity are shown, when the object is observed under true anomaly of about 186 degrees. For the true anomaly a value close to the apogee has been chosen for which the effect of the changing eccentricity value is suspected to be at maximum.

Fig.2a shows that the crosstrack offset is very close to zero, smaller than 0.5 percent for all eccentricities. The intrack offset is below three percent for eccentricities up to 0.4. For an eccentricity of 0.9 the value is still below 65 percent and reaches a value of 130 for an eccentricity close to one. The offset for the radial component starts around 100 percent and reaches a maximum of 224 percent close to an eccentricity of 0.9 before the value drops rapidly. To get a more complete picture the offsets are also evaluated at a fixed eccentricity of 0.8 as a function of the true anomaly, see Fig.2b. The eccentricity value has been chosen since it shows the largest offsets at a true anomaly of 186 degrees. In Fig.2b it can be seen, that the offsets depend where in the orbit, at which anomaly, the object is observed. The crosstrack component stays below one percent for all anomalies. The intrack component reaches a maximum offset of about 90 percent at a true anomaly of about 216 degrees before the value drops again. The radial component has a sharp rise starting from 100 percent at 180 degrees until it reaches its maximum of 225 percent at an anomaly of about 193 degrees. After that there is a slow decrease down to 200 percent before the value reaches slowly the maximum value again for true anomalies close to 270 degrees.

Alternatively the radial distance of the observed object can be estimated by the distance of the topocenter to the intersection point of the projection of the observed direction into the orbital plane with the orbit of the catalogue object, see Fig.3. With the same simulation setup as before the offsets in intrack, crosstrack and radial direction are determined. In Fig.4a the offsets are shown as a function of eccentricity for a true anomaly of 186 degrees and in Fig.4b as a function of the true anomaly for a fixed eccentricity of 0.8.

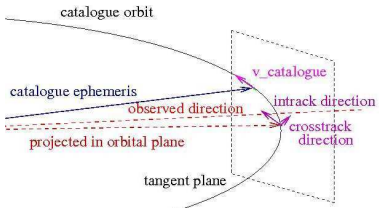

Figure 3: Catalogue and observed position provided that the radial distance of observed object is determined by the intersection of the projection of the observed direction with the catalogue orbit with intrack and crosstrack direction in tangent plane.

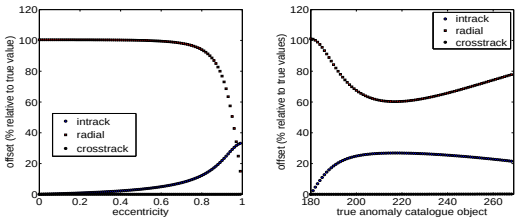

(a) *(b)*

Figure 4: Systematic offsets in percent relative to the "true" errors intrack, crosstrack and radial (NTW system) as a function of eccentricity (a) and true anomaly (b) assuming that the radial distance of observed object is determined by the intersection of the projection of the observed direction with the catalogue orbit .

Fig.4a shows that the crosstrack offset is very close to zero for all eccentricities, it is below 0.5 percent. The intrack offset is below 2.5 percent for eccentricities lower than 0.4. It rises up to 12 percent close to an eccentricity of 0.8 and reaches its maximum value of 33 percent close to one. The radial error stays around 100 percent up to eccentricities of 0.7 then it drops rapidly and reaches a minimum value of 15 percent close to one. In Fig.4b it can be seen again that the values of the offsets in intrack and radial direction depend strongly on the point on orbit at which the object is observed. The offset in crosstrack direction stays below 0.5 percent for all anomalies. The intrack offset rises up to a maximum value of 27 percent close to 217 degrees and decreases slowly for higher true anomalies. The radial component starts with an offset of 101 percent close to 180 degrees and reaches it minimum value of 61 percent at 210 degrees. For higher anomalies it rises slowly again up to 78 percent for a true anomaly close to 270 degrees.

In general the intrack and crosstrack offsets are within the same range for both methods. The radial component is better determined with the latter method especially for high eccentricities and anomalies which are not close to 180 degrees. Generally all offset values are sensitive to the specific initial conditions that have been chosen. In the actual implementation of the algorithm the offsets are projected into the tangent plane. In real observations the orientation of the projection plane is determined by the parallax.

Despite the smaller offsets in the radial component, the first method is implemented because it is computationally less intensive than the latter.

In the actual implementation of the algorithm additional quantities are determined to perform the correlation: The projection of the observed and computed velocity vectors in the tangent plane. The velocity vector of the observed object is determined using two subsequent observations within one tracklet. The angle between the direction of velocity of the observed object projected into the tangent plane and the projected velocity of the catalogue object is a sensitive value in the correlation; it reveals the tipping of the orbital planes of the observed with respect to the catalogue object's orbit.

2.2 Error assessment by means of observations

To assess the errors of the DISCOS catalogue, follow-up observation tracklets of 13 GEO objects and eight GTO objects have been evaluated. The observations have been acquired with the ZIMLAT over a period of more than four years. The verification that the different tracklets actually belong to the same objects has been performed by orbit determination. In addition the GEO objects have been correlated with DISCOS observed during the campaigns from January to March 2008 at the ESASDT have been evaluated, validation has been performed by comparing the correlations to the results of the old algorithm. The results of the correlations are illustrated for the GEO resp. GTO objects in Fig.5 resp. Fig.6. Displayed are the arc length error in degrees, the intrack and crosstrack errors (absolute values) in kilometers and the angle in degrees between the velocity direction of observed and catalogue objects.

Under the assumption of a normal distribution the following expectation values and standard deviations could be found.
The expectation values and standard deviations for the arc length error of the ZIMLAT resp. ESASDT observations in GEO are:

$$\begin{aligned} \langle E_{\text{arc\_zim}} \rangle &= 2.01 \cdot 10^{-2} \text{ degrees} \\ \sigma_{\text{arc\_zim}} &= 1.44 \cdot 10^{-2} \text{ degrees} \end{aligned} \quad (1)$$

$$\begin{aligned} \langle E_{\text{arc\_esa}} \rangle &= 3.34 \cdot 10^{-2} \text{ degrees} \\ \sigma_{\text{arc\_esa}} &= 1.50 \cdot 10^{-2} \text{ degrees} \end{aligned} \quad (2)$$

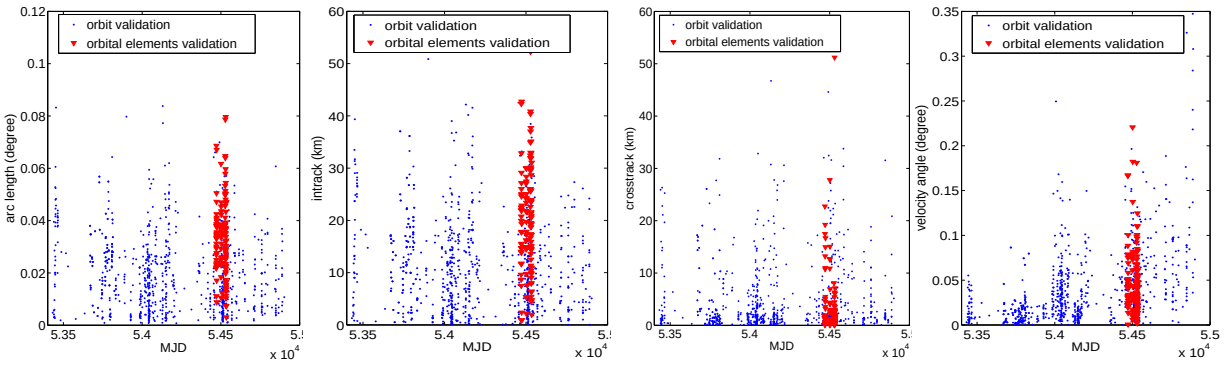

(a) *(b)* *(c)* *(d)*

Figure 5: GEO: (a) arc length error, (b) intrack error, (c) crosstrack error (both absolute values), (d) angle between velocities of observed and catalogue objects.

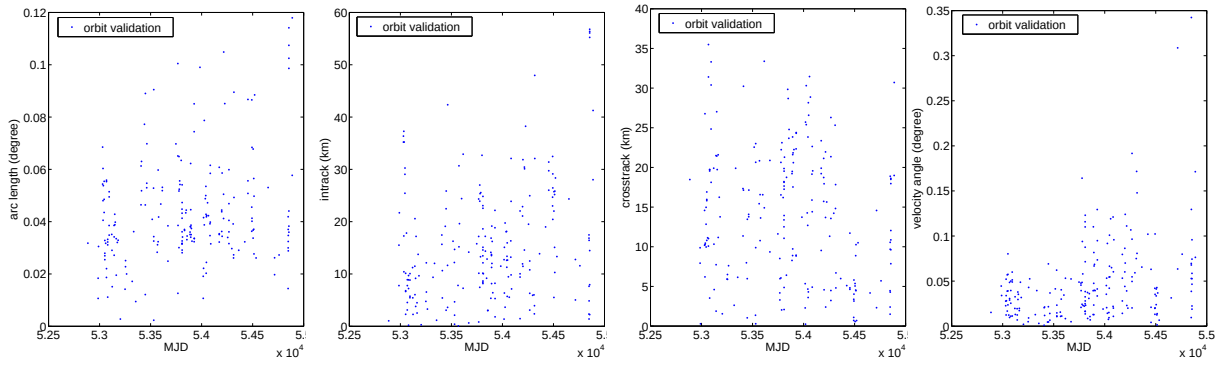

(a) *(b)* *(c)* *(d)*

Figure 6: GTO: (a) arc length error, (b) intrack error, (c) crosstrack error (both absolute values), (d) angle between velocities of observed and catalogue objects

The expectation values and standard deviations for the intrack and crosstrack errors (absolute values) of the ZIMLAT resp. ESASDT observations in GEO are:

$$\langle E_{\text{in\_zim}} \rangle = 11.14\,\text{km} \qquad \sigma_{\text{in\_zim}} = 15.36\,\text{km} \tag{3}$$

$$\langle E_{\text{cross\_zim}} \rangle = 4.80\,\text{km} \qquad \sigma_{\text{cross\_zim}} = 6.77\,\text{km} \tag{4}$$

$$\langle E_{\text{in\_esa}} \rangle = 20.23\,\text{km} \qquad \sigma_{\text{in\_esa}} = 13.55\,\text{km} \tag{5}$$

$$\langle E_{\text{cross\_esa}} \rangle = 3.87\,\text{km} \qquad \sigma_{\text{cross\_esa}} = 6.58\,\text{km} \tag{6}$$

The expectation values and standard deviations for the angle between moving directions of the ZIMLAT resp. ESASDT observations in GEO are:

$$\begin{aligned} \langle E_{\text{angle\_zim}} \rangle &= 3.93 \cdot 10^{-2}\,\text{degrees} \\ \sigma_{\text{angle\_zim}} &= 4.33 \cdot 10^{-2}\,\text{degrees} \end{aligned} \tag{7}$$

$$\begin{aligned} \langle E_{\text{angle\_esa}} \rangle &= 5.19 \cdot 10^{-2}\,\text{degrees} \\ \sigma_{\text{angle\_zim}} &= 3.94 \cdot 10^{-2}\,\text{degrees} \end{aligned} \tag{8}$$

The expectation value and standard deviation for the arc length error of the ZIMLAT observations in GTO are:

$$\begin{aligned} \langle E_{\text{arc\_zim}} \rangle &= 4.36 \cdot 10^{-2}\,\text{degrees} \\ \sigma_{\text{arc\_zim}} &= 2.06 \cdot 10^{-2}\,\text{degrees} \end{aligned} \tag{9}$$

The expectation value and standard deviation for the intrack and crosstrack error (absolute values) of the ZIMLAT observations in GTO are:

$$\langle E_{\text{in\_zim}} \rangle = 15.28\,\text{km} \qquad \sigma_{\text{zim\_in}} = 21.75\,\text{km} \tag{10}$$

$$\langle E_{\text{cross\_zim}} \rangle = 13.84\,\text{km} \qquad \sigma_{\text{cross\_zim}} = 8.35\,\text{km} \tag{11}$$

The expectation value and standard deviation for the angle between moving directions of the ZIMLAT observations in GTO are:

$$\begin{aligned} \langle E_{\text{angle\_zim}} \rangle &= 5.54 \cdot 10^{-2}\,\text{degrees} \\ \sigma_{\text{angle\_zim}} &= 7.5 \cdot 10^{-3}\,\text{degrees} \end{aligned} \tag{12}$$

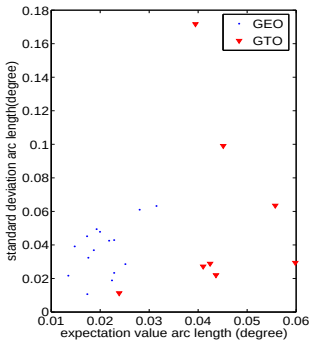

Figure 7: Standard deviation as a function of expectation value of the arc length error for 13 GEO and 8 GTO objects.

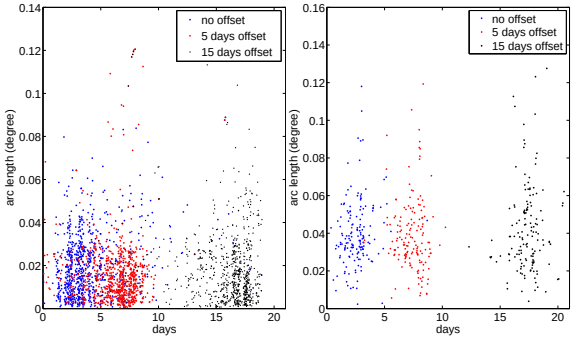

(a) *(b)*

Figure 8: Arc length error of (a) 13 GEO and (b) 8 GTO objects for time span since TLE creation.

All values are higher for GTO than for GEO objects. Surely, the systematic offsets introduced by the method of radial distance estimation are larger for higher eccentricities. Nevertheless an explanation could be that the catalogue orbits are intrinsically less accurate for GTOs [3].

Independently of this, the standard deviations of all parameters, for GTO and for GEO objects are remarkably high. They are of the same magnitude than the expectation values themselves. This effect is not introduced by a minority of the observed objects, but can be observed for all of them. In Fig.7 the standard deviation as a function of the expectation value of the arc length error for the every single GEO and GTO object is plotted.

The wide variations cannot be explained by systematic errors in the observations. Further investigation shows that the variation in the errors seem to be independent of the time span between the observation epoch and the TLE reference epoch, as it can be inferred from the Fig.8a and Fig.8b. The figures show the arc length error for the GEO and GTO objects, first by using TLEs with the reference epoch closest to the observation epoch (labeled “no offset”) and then by using TLEs which would be closest to an observation epoch shifted by five and 15 days. Unfortunately the date displayed for each object in the DISCOS catalogue is not necessarily the date when the last observation entered. To gain more insight, TLEs based on AIUB observations of objects have been generated. Fig.9 shows the arc length error for correlation with TLEs calculated at the AIUB and the DISCOS TLEs of four GEO and two GTO objects. The AIUB TLEs have been generated for each night by numerically propagating the orbit. It can be seen that the AIUB TLEs are slightly better than the DISCOS TLEs.

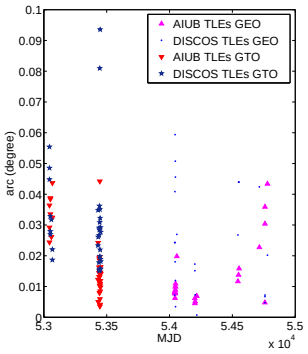

Figure 9: Arc length errors between observed and calculated position out of AIUB TLEs and DISCOS TLEs of 4 GEO and 3 GTO objects.

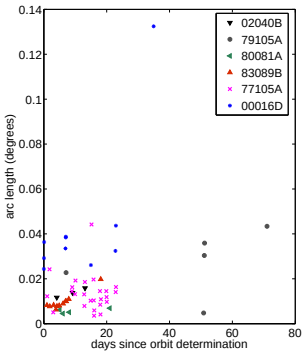

Figure 10: Arc length error between observed and calculated position of 4 GEO and 3 GTO objects as a function of time span since orbit determination.

In Fig.10 the arc length error is displayed as a function of the time span since the last observation contributing

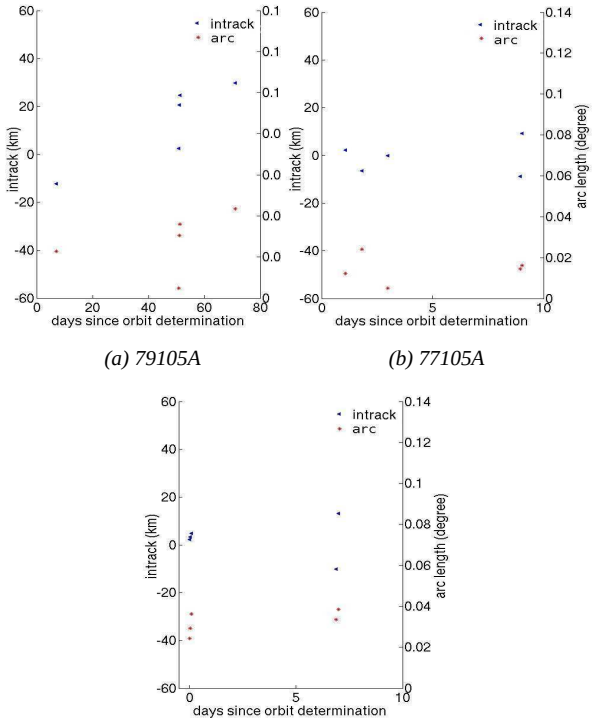

(a) 79105A *(b) 77105A*

(c) 00016D

Figure 11: Intrack and arc length error as a function of time since orbit determination for the GEO object (a) Gorizont 3 (79105A), (b) Molniya-3 (77105A) and (c) Ariane 5 R/B rocket body (00016D, GTO).

to orbit determination. The first four objects displayed in the legend of Fig.10 are the GEO, followed by one Molniya and one GTO object. There is a trend that the arc length error is increasing with the time span since the last orbit determination. Within the first days after the orbit determination the errors are below 0.02 degrees, but as time progresses, the errors increase for all objects. Fig.10 also shows, that there are short term variations, which are clearly not correlated with the time since the last observation contributed to orbit determination. This is the case especially for the Molniya-3 (77105A) object and the GTO object Ariane 5 R/B rocket body (00016D)).

To take a closer look at the short term variations, intrack errors of the GEO object Gorizont 3(79105A), the Molniya-3 (77105A) and the GTO object Ariane 5 R/B rocket body (00016D) together with the arc length error are plotted as a function of the time interval since last observation contributing to orbit determination, see Fig.11. It turns out (not displayed in the figure) that the intrack error oscillates between a minimum value, which has a negative sign, that is, the observed object is ahead of the position of the predicted position up to a maximum positive value, that is the observed object is behind the predicted position.

The arc length error is independent of the actual radial distance estimation of the observed object. All orbits have been determined with an rms of less than 0.6 arcseconds, direct radiation pressure has been estimated with a simple model for the Molniya and the GTO objects and most GEO objects but not for the orbit of Gorizont 3 (79105A). The observations, which entered the orbit determination, cover an arc length between 14 and 50 days. Further investigation is needed to explain this behaviour. It also has to be checked if these variations in the intrack component are correlated with the radial distance determination, explained in the preceding section.

3 RESULTS

3.1 ESASDT

The new algorithm for catalogue correlation has been successfully implemented in the automatic processing software of the ESASDT. The campaigns from January to March 2008 have been reprocessed with the new algorithm and compared to the results of the old algorithm. The tracklets that could be correlated with DISCOS and the uncorrelated tracklets are shown in Fig.12. For GEO objects roughly the same results have been achieved, since the old algorithm has been used to assess the catalogue errors, which have been used in the correlation with the new algorithm. Three GEO objects correlated with the catalogue by the old algorithm are not correlated with the new algorithm. It can be shown that the ephemerides position is too far away from the observed position to be a valid correlation. But the comparison of Fig.12a and Fig.12b clearly shows that overall more objects could be correlated. This is especially the case for faint objects, which consist mostly of GTO objects or objects with non-vanishing eccentricity. In Fig.13 the mean motion distribution in revolutions per day for a circular orbit determination is shown. The comparison of the results of the old algorithm Fig.13a with the new algorithm Fig.13b reveals, that a lot more objects with a mean motion of unequal one could be correlated. The determination of a circular orbit based on tracklets of objects on orbits with non-vanishing eccentricity can result in revolutions per day unequal to one.

Since the objects that are observed by the AIUB at the ESASDT are mostly GTOs or other high eccentricity objects, a correlation of the internal catalogue with the old algorithm cannot be performed before a six parameter orbit is determined. The new algorithm

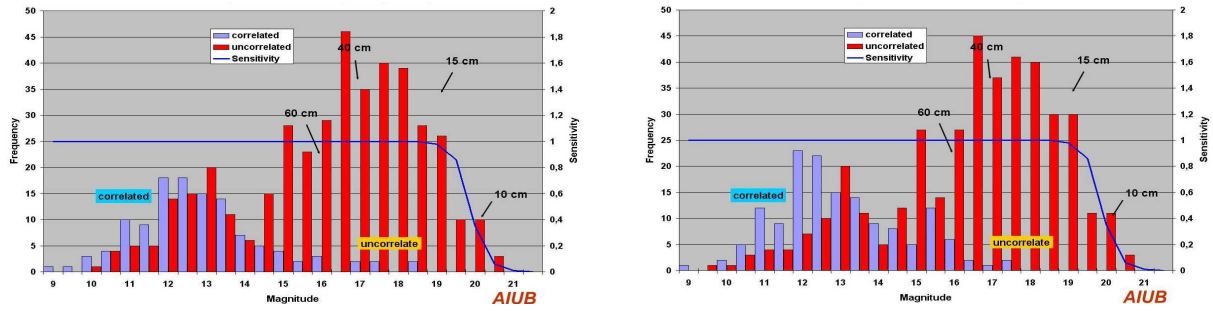

(a) old algorithm *(b) new algorithm*

Figure 12: Magnitude histogram: Correlated and uncorrelated tracklets of the campaigns January 2008 to March 2008. (a) with the old catalogue correlation algorithm, (b) with the new catalogue correlation algorithm.

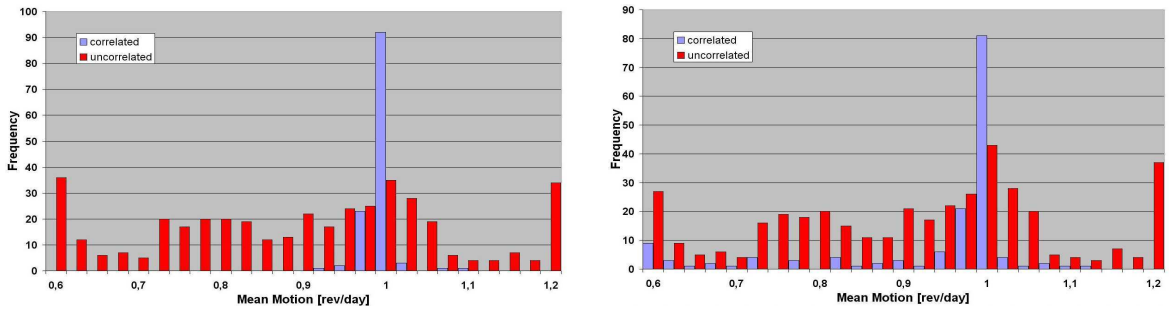

(a) old algorithm *(b) new algorithm*

Figure 13: Mean motion histogram (circular orbits): Correlated and uncorrelated tracklets of the campaigns January 2008 to March 2008. (a) with the old catalogue correlation algorithm, (b) with the new catalogue correlation algorithm.

allows to correlate about 90% of the observed follow-up tracklets of objects for which internal TLEs exist in real time without inferring a circular orbit. For the others the errors do not allow a unique correlation. But a strong indication can be given, which of the possibly many objects in the field of view is most likely the object follow-up. Surveys for detection of new objects also benefit because with the new algorithm GEO and GTO objects, known from internal or external catalogues can be identified correctly.

3.2 ZimSMART

First tests in the experimental processing of ZimSMART data were performed. Both ASTRA clusters (longitude 28 and 19 degree east) consisting of four resp. five satellites were observed and a correlation was performed. With the tracklets that could be correlated an orbit was determined. As Reto Musci in [4] pointed out, the single tracklets can be uniquely assigned to each other via orbit determination, when the rms in the orbit determination is below 2.5 arcseconds. This is even the case for objects in very similar orbits like objects in clusters.

After the actual correlation of the different tracklets, a superstructure of the algorithm is passed through. An additional consistency check is performed: A catalogue object is not allowed to be correlated with more than one tracklet on the same frame. In case of a conflict, only the correlation with the smallest error values is kept, all others are rejected.

The results of the correlations are shown in Tab.1 for the first cluster (longitude 28 degrees east) and in Tab.2 for the second cluster (longitude 19 degrees east). The tracklets (named T_..), which correlated with one object, their observation epoch (MJD) and rms (arcseconds) from the orbit determination of those tracklets are shown. A hyphen indicates, that no more objects was detected on the frames of the observation series, a “no cor” indicates, that there was at least one other tracklet detected in the series, which did not correlate.

In the first cluster (Tab.1) three of the four ASTRA satellites could be correlated and the orbit determination was successful. In the second cluster (Tab.2) four of the five ASTRA satellites could be correlated. The orbit determination has been successful.

Table 1: ASTRA Cluster at longitude 28°: Correlation of observed tracklets (T_..) at three different epochs [MJD] with rms of the orbit determination; "no corr" means another object was on the frames, which could not be correlated, "-" means no other object was detected on the frames.

COSPAR	54887.876	54887.961	54888.153	rms
00054A	T_3	T_4	T_1	0.62"
00081A	T_1	T_1	T_2	1.41"
98050A	T_2	no cor	-	
01025A	T_4	T_3	T_3	0.58"

Table 2: ASTRA Cluster at longitude 19°: Correlation of observed tracklets (T_..) at three different epochs [MJD] with rms of the orbit determination; "no corr" means another object was on the frames, which could not be correlated, "-" means no other object was detected on the frames.

COSPAR	54866.052	54866.803	54867.185	rms
96021A	T_1	T_6	T_3	2.01"
06012A	T_2	T_1	T_2	1.41"
99033A	T_3	T_3	T_5	1.41"
97076A	T_4	T_2	T_6	0.43"
07016A	-	T_5	no cor	

In both cases orbit determination was also performed with all the tracklets that could not be correlated and the objects, for which only one tracklet was found. The orbit determination was not successful in all these cases. This means, the remaining tracklets do not belong to the missing objects.

4 CONCLUSION

A new algorithm for catalogue correlation has been developed and implemented. This new algorithm correlates observation tracklets by comparing observed positions and velocities with catalogue ephemerides. The radial distance is approximated for the observed objects, because it is not provided directly by optical observations but can only be inferred from orbit determination. The new algorithm is independent of a first orbit determination.

Since official catalogues as DISCOS do not provide any covariance information, the catalogue errors had to be assessed by comparing the catalogue orbits with observations. The errors for GTO objects are generally higher than for GEO objects. It has been shown, that variations in the errors of both GEO and GTO objects do not correlate with the time interval since the epoch of the TLEs. But it is shown with TLEs based on AIUB observations, that the errors do correlate with the time interval since new observations are available and a new orbit is determined. This suggests, not surprisingly, that the epoch displayed in the TLEs does not correspond to the point in time, when the last observations entered orbit determination. Furthermore short term variations have been found, which are independent of the time since last orbit determination. Further investigation is needed.

The new algorithm has been implemented in the ESASDT processing and is used in the experimental processing of ZimSMART data. With the new algorithm tracklets of GEO and GTO objects of surveys and follow-up observations can be correlated in real time with the external DISCOS catalogue and with an internal orbit catalogue. This is a major improvement in the processing of the ESASDT. The additional environment, which excludes correlations of one and the same catalogue object with two or more tracklets, which are on the same frames, makes it possible to correlate the majority of observations of objects which are in very similar orbits as it is the case in clusters.

5 ACKNOWLEDGMENT

The observations from the ESASDT were acquired under ESA/ESOC contracts 15836/01/D/HK and 17835/03/D/HK.

The work was supported by the Swiss National Science Foundation through grants 200020-109527 and 200020-122070.

6 REFERENCE

[1] G. Beutler. *Methods of Celestial Mechanics*. two volumes. Springer-Verlag, Heidelberg, 2005. ISBN: 3-540-40749-9 and 3-540-40750-1.

[2] R. Musci. *Identification and Recovery of Objects in GEO and GTO to Maintain a Catalogue of Orbits*. Astronomical Institute, University of Bern, 2006. PhD thesis.

[3] D. Vallado and W. McCain. *Fundmentals of Astrodynamics and Applications*. Microcosm Press, El Sugunda, California, 2001. ISBN 0-7923-6903-3.

[4] R. Musci, T. Schildknecht, T. Flohrer, and G. Beutler. Concept for a Catalogue of Space Debris in GEO. In *Proceedings of the Fourth European Conference on Space Debris, pp. 601-606, ESOC, Darmstadt, Germany, 18-20 April 2005*, 2005.